

Extension to Imaginary Chemical Potential in a Holographic Model

[†]Kazuo Ghoroku¹, [†]Kouji Kashiwa², Yoshimasa Nakano³,
[§]Motoi Tachibana⁴ and [‡]Fumihiko Toyoda⁵

[†]Fukuoka Institute of Technology, Wajiro, Fukuoka 811-0295, Japan

[§]Department of Physics, Saga University, Saga 840-8502, Japan

[‡]Faculty of Humanity-Oriented Science and Engineering, Kinki University,
Iizuka 820-8555, Japan

Abstract

We extend a bottom up holographic model, which has been used in studying the color superconductivity in QCD, to the imaginary chemical potential (μ_I) region, and the phase diagram is studied on the μ_I -temperature (T) plane. The analysis is performed for the case of the probe approximation and for the background where the back reaction from the flavor fermions are taken into account. For both cases, we could find the expected Roberge-Weiss (RW) transitions. In the case of the back-reacted solution, a bound of the color number N_c is found to produce the RW periodicity. It is given as $N_c \geq 1.2$. Furthermore, we could assure the validity of this extended model by comparing our result with the one of the lattice QCD near $\mu_I = 0$.

¹gouroku@fit.ac.jp

²kashiwa@fit.ac.jp

³ynakano@kyudai.jp

⁴motoi@cc.saga-u.ac.jp

⁵f1toyoda@jcom.home.ne.jp

1 Introduction

The holographic approach based on the string/gauge duality is a powerful method to study various thermo-dynamical and non-perturbative properties of the Yang-Mills theory especially when the chemical potential (μ) of the fundamental fermions plays an important role. Various results have been obtained in such cases and they could give us many kinds of insight into the phase diagram of QCD. (See for example [1, 2, 3, 4].)

On the other hand, many non-perturbative investigations in QCD have been performed by the lattice gauge theory. However, the analysis has been restricted to the case of the imaginary chemical potential, μ_I , to avoid the sign problem of the fermion determinant (See for example [5, 6]). In QCD with μ_I , on the other hand, the Roberge-Weiss (RW) phase transition and its periodicity with respect to μ_I have been pointed out as a remarkable point [7]. This observation is understood from the periodicity of the partition function. It would be meaningful to see how this point is realized in the holographic approach to make clear the validity of the holographic approach.

Ten years ago, however, such a holographic investigation has been given based on the Euclidean space-time geometry [8, 9, 11]. In the Ref. [8], the periodic RW transition has been shown by adding the two-form Kalb-Ramond field B in the D3/D7-brane system of the type IIB model. After that, also in the D4/D8-brane system in IIA model, similar analysis has been done in Ref. [9], and also in Ref. [10, 11] in a slightly different method. In these approaches, the essential point is the introduction of the B field with $dB=0$ and its potential $V_A(\alpha)$, where α corresponds to the phase of the Polyakov loop [12, 13]. It is introduced as ¹

$$\alpha = \int_{D_2} \frac{B}{2\pi\alpha'}. \quad (1.1)$$

And this parameter α discriminates the periodic vacua in the deconfinement phase with spontaneously broken Z_N symmetry. On the other hand, μ_I comes from the bulk U(1) gauge field $F(= F_{\mu\nu}dx^\mu \wedge dx^\nu)$, and it appears in the theory being combined with α as

$$\alpha - \frac{\mu_I}{T} = \int_{D_2} \left(F + \frac{B}{2\pi\alpha'} \right). \quad (1.2)$$

The important point is that the potential $V_A(\alpha)$ is periodic under $\alpha \rightarrow \alpha + 2\pi/N_c$ due to the gauge symmetry of the boundary SYM theory [7] ². As a result, the total effective potential, the sum of $V_A(\alpha)$ and the probe action, is also periodic under $\mu_I/T \rightarrow \mu_I/T + 2\pi/N_c$, since a finite shift of μ_I/T can be absorbed into α as understood from (1.2). The role of μ_I in the probe action is to control the minimum of the effective total potential of α as seen in the RW phase transition [7, 8].

¹The disc D_2 is a part of the black hole geometry considered here.

²See also the appendix A.

The purpose of this paper is to extend the analysis performed for μ_I in the top down models to a bottom up model which has been used to study the color superconductivity in QCD [14, 15, 16]. Through the extension, we could get phase diagrams for our model in the region of μ_I with RW transitions. And an implication of our holographic model is discussed. Especially, when the back-reaction of flavor fermions is included, we find a μ_I -dependent critical curve of confinement/deconfinement transition. In this case, we could show the usefulness of a simple continuation, $\mu \rightarrow i\mu_I$, in terms of the critical curve obtained for real μ . This usefulness is supported by the fact that we can set as $\alpha = 0$ near $\mu_I = 0$.

In the next section, the extended bottom up model is proposed and the actions are estimated for confinement and deconfinement phases. In Sec.3, the RW transitions are investigated in the probe approximation, and for the back reacted case. Then the phase diagrams are given. In Sec. 4, the validity of the continuation near $\mu = 0$ is discussed by comparing the critical curve near $\mu = 0$ for the holographic model and the one of the dual QCD theories. A problem related to a wide periodicity of the potential of μ_I is discussed in Sec.5. Our summary is given in the final section.

2 A bottom up model

A bottom up model, which is used before to study the superconductivity of QCD [14], is given in a slightly modified form of the following action for the Euclidean space-time to investigate QCD with the imaginary chemical potential.

$$S = S_{\text{bu}} + S_{F(4)} , \quad (2.1)$$

where the first term is given as

$$S_{\text{bu}} = \int d^6x \sqrt{-g} (\mathcal{L}_{\text{Gravity}} + \mathcal{L}_{\text{CSC}}) , \quad (2.2)$$

$$\mathcal{L}_{\text{Gravity}} = \frac{1}{2\kappa_6^2} \left(\mathcal{R} + \frac{20}{L^2} \right) , \quad (2.3)$$

$$\tilde{\mathcal{L}}_{\text{CSC}} = -\frac{1}{4}\tilde{F}^2 - |D_\mu \psi|^2 - m^2|\psi|^2 , \quad (2.4)$$

$$\tilde{F}_{\mu\nu} = \partial_\mu A_\nu - \partial_\nu A_\mu + \frac{B_{\mu\nu}}{2\pi\alpha'} , \quad D_\mu \psi = (\partial_\mu - iqA_\mu)\psi . \quad (2.5)$$

This action S_{bu} is proposed as a model dual to the SYM theory with strongly interacting flavor fermions with the chemical potential μ when the space-time is Lorentzian and $B_{\mu\nu}$ is neglected. In the gravitational action $\mathcal{L}_{\text{Gravity}}$, the scale L denotes the AdS radius.

In the present case, the theory is set in the Euclidean space-time. It is obtained by the Wick rotation of both the time and fields. Furthermore, the Kalb-Ramond field is added through $\tilde{F}_{\mu\nu}$. This form of $\tilde{F}_{\mu\nu}$ is implied from the D-brane action. And ψ denotes a charged scalar, which is supposed to be dual to the cooper pair of the color charged fermions. Its baryon number charge is assigned as q . We could show that there is no non-trivial solution for ψ in the region of small and negative μ^2 [14]. Since μ is imaginary for negative μ^2 , we can neglect ψ hereafter because we are considering the case with the imaginary chemical potential.

Then, the system can be solved by setting as $\tilde{A}_0 = \tilde{\phi}$ where \tilde{A}_μ is defined by

$$\tilde{F}_{\mu\nu} \equiv \partial_\mu \tilde{A}_\nu - \partial_\nu \tilde{A}_\mu. \quad (2.6)$$

This replacement can be justified since B is introduced with $dB = 0$. In this case, we will find the same form of equations of motion with the one of the real μ theory given in the Lorentzian space-time. However, in the present case, we must notice that the solution $\tilde{\phi}$ is not simply a chemical potential but a combination of the chemical potential and α as found from (1.2). This fact implies that we can obtain the solutions with $\tilde{\phi}$ for μ_I from the one of the real μ by a replacement, $\mu/T \rightarrow i(\mu_I/T - \alpha)$.

As for the action $S_{F_{(4)}}$, this is necessary to study the potential of α . Its explicit form and an effective potential of the B field is given in 2.2.

2.1 Bulk solutions

As mentioned above, neglecting $\tilde{\phi}$, we can obtain solutions with the imaginary chemical potential μ_I . We give three solutions dual to the ground states of the pure YM fields, and they are compared. Two of them are the solutions of L_{Gravity} only, then they are independent of μ . The third solution is constructed by considering the back-reaction from \tilde{F}^2 .

(1) AdS soliton solution: This represents the low temperature confinement phase, and it is given as

$$ds^2 = r^2(\delta_{\mu\nu}dx^\mu dx^\nu + f(r)dw^2) + \frac{dr^2}{r^2 f(r)}, \quad (2.7)$$

where

$$f(r) = 1 - \left(\frac{r_0}{r}\right)^5, \quad r_0 = \frac{2}{5R_w}, \quad (2.8)$$

and $2\pi R_w$ denotes the compactified length of w .

(2) The AdS-Schwarzschild solution: This solution corresponds to the high temperature deconfinement phase,

$$ds^2 = r^2(fdt^2 + \Sigma_i^3(dx^i)^2 + dw^2) + \frac{dr^2}{r^2 f(r)}, \quad (2.9)$$

where

$$f(r) = 1 - \left(\frac{r_0}{r}\right)^5, \quad r_0 = \frac{2}{5R_w}, \quad (2.10)$$

(3) Reissner-Nordstrom (RN): In this case, the back-reaction of flavor is taken into. It represents the high temperature deconfinement phase.

The background of RN is given as the solution of the following action

$$S_G = \int d^6x \sqrt{-g} \left\{ \frac{1}{2\kappa_6^2} \left(\mathcal{R} + \frac{20}{L^2} \right) - \frac{1}{4} \tilde{F}^2 \right\}, \quad (2.11)$$

which includes the flavor part. We get the following RN solution,

$$ds^2 = r^2(gdt^2 + \Sigma_i^3(dx^i)^2 + dw^2) + \frac{dr^2}{r^2g(r)}, \quad (2.12)$$

$$g = 1 - \left(1 - \frac{3\tilde{\mu}^2}{8r_+^2}\right) \left(\frac{r_+}{r}\right)^5 - \frac{3\tilde{\mu}^2 r_+^6}{8r^8} \quad (2.13)$$

$$\tilde{A}_0 = \tilde{\phi} = \tilde{\mu} \left(1 - \frac{r_+^3}{r^3}\right) \quad (2.14)$$

Here r_+ denotes the horizon of the charged black hole, and the temperature is given as

$$T = \frac{1}{4\pi} \left(5r_+ + \frac{9\tilde{\mu}^2}{8r_+}\right). \quad (2.15)$$

Here, $\tilde{\mu}$ is defined by

$$-\frac{\tilde{\mu}}{T} = \int_{D_2} \tilde{F} = \int_{D_2} \left(F + \frac{B}{2\pi\alpha'}\right) = \alpha - \frac{\mu_I}{T}. \quad (2.16)$$

The action densities for these solutions, (1) AdS-Soliton (2) AdS-Schwartzchild and (3) RN, are given as

$$S_1/V_3 = -r_0^5 v_2 = -r_0^5 \frac{4\pi}{5r_0} \frac{1}{T} \quad (2.17)$$

$$S_2/V_3 = -r_0^5 v_2 = -r_0^5 \left(\frac{4\pi}{5r_0}\right)^2 \quad (2.18)$$

$$S_3/V_3 = -r_+^5 \left(1 - \frac{3\tilde{\mu}^2}{8r_+^2}\right) v_2 = -r_+^5 \left(1 - \frac{3\tilde{\mu}^2}{8r_+^2}\right) \frac{4\pi}{5r_0} \frac{1}{T} \quad (2.19)$$

where $v_2 = \int_0^\beta d\tau \int dw$, $V_3 = \int dxdydz$. In $\mu_I - T$ plane, we can find the phase diagram by comparing the above three actions. We find that the phase of the solution (2) is not realized when the solution (3) is added.

2.2 Potential of Kalb-Ramond field

Consider the Kalb-Ramond field B , which is introduced in terms of α which is defined by (1.1). The present bottom up model would be related to D4/D8 model of type IIA string. Then the bulk action, which could provide the potential of α , might be given as

$$S_{F_{(4)}} = -\frac{1}{2\kappa_6^2} \left(\int d^6x \sqrt{g} \frac{1}{12} F_{(4)}^2 - \int B \wedge F_{(4)} \right). \quad (2.20)$$

In the RN background, (2.12)-(2.15), this action is estimated for a constant field F_{123w} and α . We obtain

$$S_{F_{(4)}} = -\frac{V_4}{2\kappa_6^2} \left(\frac{\beta}{6r_+^3} F_{123w}^2 - \alpha F_{123w} \right). \quad (2.21)$$

where $V_4 = \int d^3x dw = \beta V_3$, $V_3 = \int dx^3$, and r_+ is used as the lower limit of the integration of r as $\int_{r_+}^{\infty} dr$. It should be replaced by r_0 in the case of solutions (1) and (2). Solving the equation of motion of F_{123w} , we find the solution as $F_{123w} = 3r_+^3 \alpha / \beta$. Then the potential is obtained as

$$S_{F_{(4)}}/V_3 \equiv V_A = \frac{1}{2\kappa_6^2} \frac{3r_+^3}{2} \alpha^2. \quad (2.22)$$

Due to the gauge symmetry of the dual SYM theory, the above result should be written as

$$V_A = \min_{n \in \mathbb{Z}} \frac{1}{2\kappa_6^2} \frac{3r_+^3}{2} \left(\alpha - \frac{2\pi n}{N_c} \right)^2. \quad (2.23)$$

3 Roberge-Weiss transitions

3.1 Probe approximation

In the probe approximation, the gauge term \tilde{L}_{CSC} is treated as the probe for the background given by the gravitational part. In this case, the background actions are given by S_1 and S_2 , and we find the critical line of confinement/deconfinement by comparing the two bulk actions. Then, the critical line is found as

$$T = \frac{5r_0}{4\pi}. \quad (3.1)$$

This is independent of μ_I , then the critical line is common to the case of real μ . The probe part defined by (2.4) is solved under these backgrounds. The equations of motion of $\tilde{\phi}$ is given by the ansatz, $\tilde{A} = \tilde{A}_\mu dx^\mu = \tilde{\phi}(r) dt$.

In the confinement phase, the background is given by the solution (1), and the equation for $\tilde{\phi}$ is given as

$$\tilde{\phi}'' + \left(\frac{4}{r} + \frac{f'}{f} \right) \tilde{\phi}' = 0. \quad (3.2)$$

We find that the allowed solution of this equation is $\tilde{\phi} = \text{const.}$. This solution gives no contribution to the free energy. On the other hand, the Kalb-Ramond field has no meaning in the confinement phase. So there is no new phase transition in this phase.

An interesting phenomenon is observed in the deconfinement phase with the background of the solution (2). In this case, we have the equation,

$$\tilde{\phi}'' + \frac{4}{r}\tilde{\phi}' = 0. \quad (3.3)$$

This equation is solved as

$$\tilde{\phi} = \tilde{\mu} \left(1 - \frac{r_0^3}{r^3} \right). \quad (3.4)$$

This solution provides a non-trivial contribution to the free energy as shown below. The probe action is given as

$$S_{CS}^E = - \int dx^6 \sqrt{-g} \left(-\frac{1}{4} \tilde{F}^2 \right) \quad (3.5)$$

$$= \int dx^5 \int_{r_0}^{\infty} dr \frac{r^4}{2} (\tilde{\phi}')^2 \quad (3.6)$$

$$= \int dx^3 V_f, \quad (3.7)$$

where

$$S_{CS}^E/V_3 = V_f = \frac{3}{2} \left(\frac{4\pi}{5} \right)^3 T \tilde{\mu}^2. \quad (3.8)$$

Then $\tilde{\mu}$ is replaced to μ_I and α by (2.16), and we obtain

$$V_f = \frac{3}{2} \left(\frac{4\pi T}{5} \right)^3 (\alpha - \mu_I/T)^2. \quad (3.9)$$

Now, from this V_f and (2.23) where r_+ is replaced by $r_0 (= 4\pi T/5)$, we find

$$V_{\text{eff}} = V_A + V_f(\alpha) = \min_{n \in \mathbb{Z}} \frac{1}{2\kappa_6^2} \frac{3}{2} \left(\frac{4\pi T}{5} \right)^3 \left(\alpha - \frac{2\pi n}{N_c} \right)^2 + \frac{3}{2} \left(\frac{4\pi T}{5} \right)^3 (\alpha - \mu_I/T)^2. \quad (3.10)$$

From this effective potential we could see the Roberge-Weiss transition for the state defined by the value of α . An example of this transition is read from the Fig., 1 in which we can see the transition from $\langle \alpha \rangle = 0$ to $\langle \alpha \rangle = 2\pi/3$ vacuum state, namely from the phase (b0) to (b1) in the Fig. 2. The resultant phase-diagram obtained from the above V_{eff} is shown in the Fig. 2. Here, the relative ratio of the probe term and the B term V_A is set by the relation $1/2\kappa_6^2 = 10$ for the simplicity.

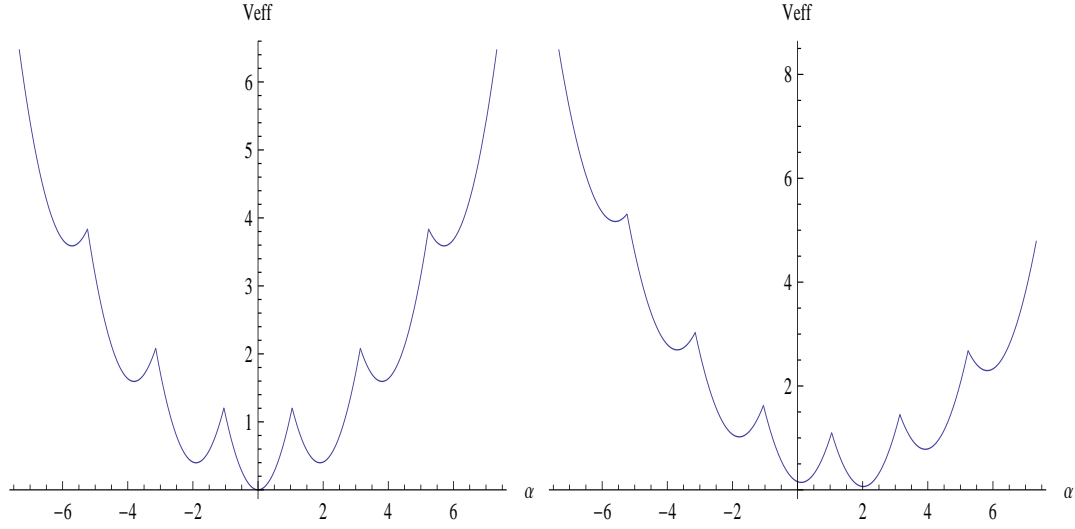


Fig. 1: V_{eff} for $\mu_I/T = 0$ (left) and $\mu_I/T = 0.6a$ (right).

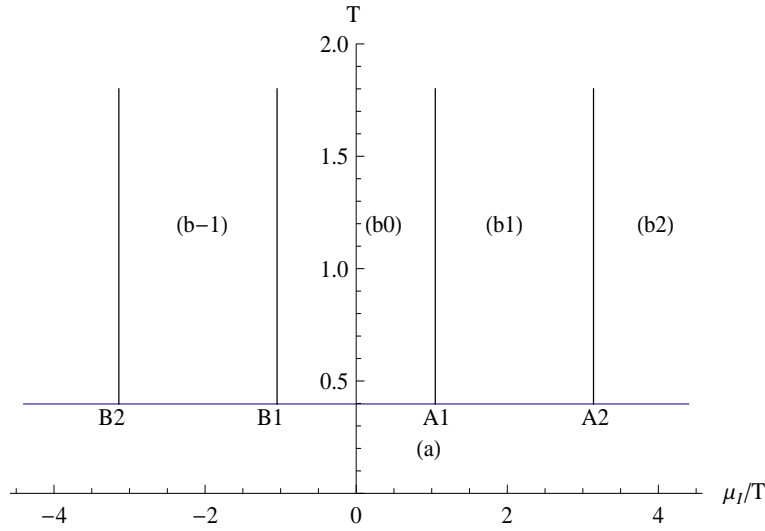


Fig. 2: Phase diagram for probe approximation. The horizontal critical line separates the confinement and deconfinement phases. In the large T deconfinement phase, the RW transitions are shown by the vertical critical lines. The points $A_1 \sim B_2$ represent tri-critical points.

Finally, we give an effective potential under the quenched approximation of the gauge field configurations which provide the real Polyakov loop. This potential is obtained from (3.10) by considering the functions at $\alpha = 2\pi n$ where $n \in \mathbb{Z}$, and it is found by picking up the minimum parts,

$$V_{\text{eff}}^{(0)} = \min_{n \in \mathbb{Z}} \frac{3}{2} \left(\frac{4\pi T}{5} \right)^3 (2\pi n - \mu_I/T)^2. \quad (3.11)$$

This potential has the period 2π with respect to μ_I/T as expected, and it is shown in the Fig. 3. This period could be understood from the phase of the boundary condition imposed on the fundamental fermions of the theory. In the present article, this potential is not used, however, this periodicity is seen for example in the calculation of the chiral condensate in the gauge configurations of the real Polyakov loops [5, 6]. On this point, the discussion is given more in the Sec. 5.

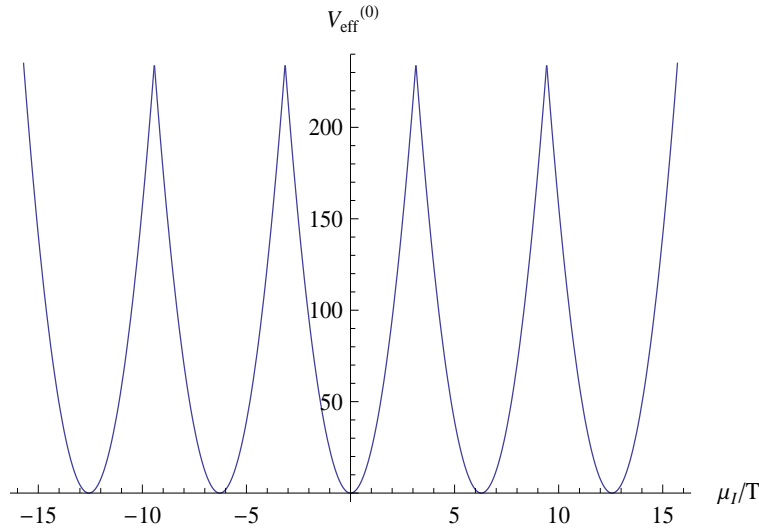


Fig. 3: $V_{\text{eff}}^{(0)}$

3.2 Back-reacted case

When the back-reaction of the flavor part is taken into account, the deconfinement background is replaced by the RN solution (3) since $S_3 < S_2$. The action S_3 is given in (2.19). We notice the $\tilde{\mu}$ dependence of S_3 is also comes from r_+ . Actually, by using (2.15), r_+ is written as

$$r_+ = \frac{2\pi T}{5} \left(1 + \sqrt{1 - \frac{45\tilde{\mu}^2}{8/(2\pi T)^2}} \right). \quad (3.12)$$

This solution is useful for $|\tilde{\mu}|/T < \sqrt{32\pi^2/45} (= 2.65)$ due to the reality of r_+ . For $|\tilde{\mu}|/T > \sqrt{32\pi^2/45}$, the system becomes unstable and decays to the stable confinement phase expressed by the solution (1), the AdS-Soliton background.

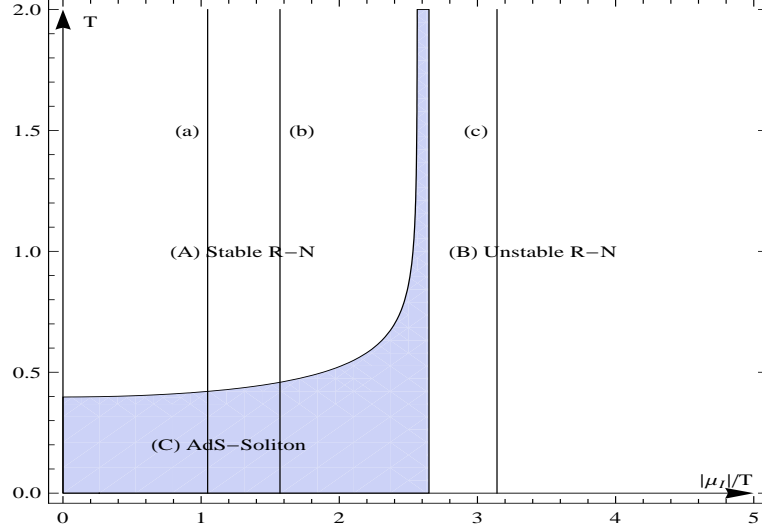


Fig. 4: Phase diagram of the back reacted case for $r_0 = 1$ and $\alpha = 0$. The lines (a), (b) and (c) represent $|\mu_I|/T = \pi/3, \pi/2$, and π respectively.

To observe the RW transitions, it is helpful to see the phase diagram for $\alpha = 0$, namely for $\tilde{\mu} = \mu_I$. This diagram is obtained by comparing S_3 with S_1 for $\alpha = 0$, and it is shown in the Fig. 4. The unstable region of solution (3) mentioned above is shown by the region (B) in this figure for $\alpha = 0$, and the regions (A) for Reissner-Nordstrom deconfinement phase and (C) for AdS soliton confinement phase are shown. Since the region (C) must be replaced by the confinement phase of (B), then the deconfinement region (A) is restricted to the definite region of $|\mu_I|/T$, $|\mu_I|/T \leq \sqrt{32\pi^2/45}$, as mentioned above. This restriction comes from the back-reaction.

Now we study the RW transitions in the deconfinement phase of region (A) by reviving α . In the present case, the effective potential is given as

$$V_{\text{eff}} = V_A + V_f^{\text{RN}} = \min_{n \in \mathbb{Z}} \frac{1}{2\kappa_6^2} \frac{3r_+^3}{2} \left(\alpha - \frac{2\pi n}{N_c} \right)^2 + V_f^{\text{RN}} \quad (3.13)$$

The first term V_A is obtained in (2.23) for the background of RN, and the second term is given as

$$S^{\text{RN}} = \frac{1}{2\kappa_6^2} \int d^6x \sqrt{-g} \left\{ \mathcal{R} + \frac{20}{L^2} - \frac{1}{4} \tilde{F}^2 \right\} = \int dx^3 V_f^{\text{RN}}. \quad (3.14)$$

Using (2.19), we find

$$V_f^{\text{RN}} = -\frac{1}{2\kappa_6^2} r_+^5 \left(1 - \frac{3\tilde{\mu}^2}{8r_+^2} \right) \frac{4\pi}{5r_0} \frac{1}{T}, \quad (3.15)$$

This potential is the part dual to the combined system of SYM fields and flavor fermions with an imaginary chemical potential μ_I .

Here, we notice that also V_A depends on $\tilde{\mu}$ through r_+ . This fact can be interpreted as a kind of the back-reaction to the Kalb-Ramond potential from the flavor fermions. In order to understand this back-reaction, we restrict the region of $|\mu_I|$ to the region of small $|\mu_I/T - \alpha|$. Then we can expand V_{eff} in the series of $-(\mu_I/T - \alpha)^2$. The expanded potential is retained up to the order of $|\mu_I - \alpha/\beta|^2$, and we obtain

$$V_A = \min_{n \in \mathbb{Z}} \frac{1}{2\kappa_6^2} \left(\frac{64\pi^3}{125} - \frac{27\pi}{50} \left(\alpha - \frac{\mu_I}{T} \right)^2 \right) T^3 \left(\alpha - \frac{2\pi n}{N_c} \right)^2 + \dots \quad (3.16)$$

$$V_f^{\text{RN}} = \frac{1}{2\kappa_6^2} \left(-\frac{1024\pi^5}{3124} + \frac{96\pi^3}{125} \left(\alpha - \frac{\mu_I}{T} \right)^2 \right) T^3 + \dots \quad (3.17)$$

We find that this result is almost equal to the probe approximation except the point that the coefficient of V_A is slightly modified. In fact, we can see a similar behavior of the potential to the one of the probe approximation. Then we could find the expected RW transitions in this case also. Furthermore, the qualitative behaviors of the potential are maintained even if the full form of potential is used. So we show here the RW transitions in terms of the full form of potential.

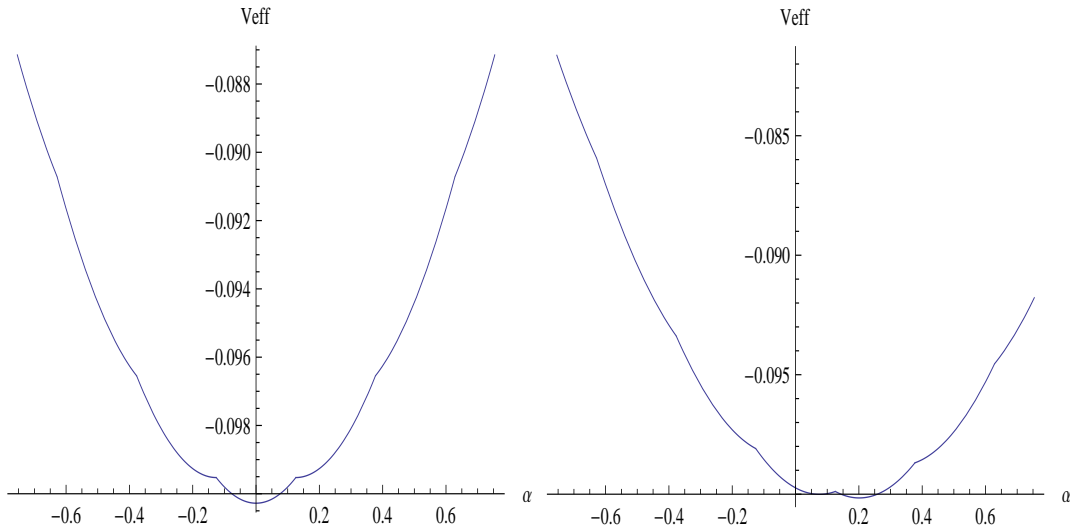


Fig. 5: Full form of V_{eff} for RN back-reacted case. Left is for $\mu_I/T = 0$, and right is for $\mu_I/T = 0.6a$ with the period of $a = 2\pi/25$.

In the Fig. 5, the effective potential with two values of μ_I/T are shown to see the RW transition from $\langle \alpha \rangle = 0$ to $\langle \alpha \rangle = a$ with the period a , which should be set as $2\pi/N_c$. It is easy to find other periodic transitions. The resultant phase diagram with the RW transitions is shown in the Fig. 6.

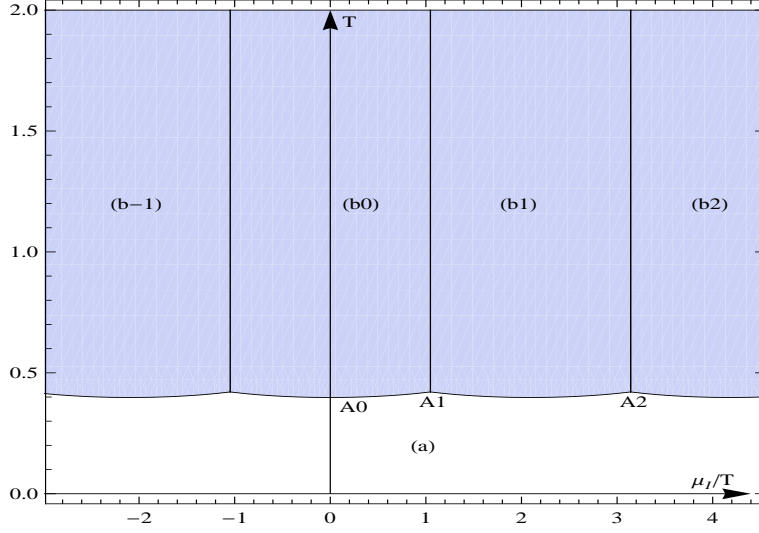


Fig. 6: Phase diagram for RW transitions under the back reacted background solution for $N_c = 3$. In the RN deconfinement phase, the phases are separated by the vertical critical-lines to the regions, (b-1) \sim (b2) for $\langle\alpha\rangle = -2\pi/3, 0, 2\pi/3, 4\pi/3$. The area (a) corresponds the AdS soliton confinement phase. The points A_1 and A_2 represent the tri-critical points.

Here, we should notice that the periodicity of μ_I/T in V_{eff} implies $|\mu_I/T| < \pi/N_c$. This and the constant, $|\mu_I|/T \leq \sqrt{32\pi^2/45}$, given above leads to the constraint,

$$N_c > 1.18. \quad (3.18)$$

In spite of the fact that N_c must be a large integer to justify the holographic approach, we are allowed to use the holography up to $N_c = 2$ at this stage.

4 Comparison with QCD near $\mu = 0$

As shown above, the μ dependent critical line obtained for real μ can be continued to the imaginary μ region and used there. The form of the critical line near $\mu = 0$ is given as [17],

$$\frac{T}{T_0} = 1 - a \left(\frac{\mu}{T_0} \right)^2 + \dots, \quad (4.1)$$

where T_0 denotes the critical temperature at $\mu = 0$, and a is a dimensionless constant, which depends on the parameters of the theory. It has been obtained also in the lattice QCD for $\mu^2 < 0$ without bothering with the sign problem. Then it is meaningful to compare the result obtained in lattice QCD with the holographic result given here.

For the probe approximation, we find $a = 0$ since the critical line is independent of μ . So we consider the RN background case, where the μ -dependent critical curve is obtained from the equation $S_1 = S_3$. And we find

$$a = \frac{15}{32\pi^2} = 0.0475. \quad (4.2)$$

In the lattice QCD, the coefficient is obtained by the form

$$a = \kappa N_c^2. \quad (4.3)$$

For confinement transition, we find many simulation results. We pick up several examples, to compare with the holographic result, where N_c is however assumed to be large. The examples of estimations of κ from lattice QCD data in the $2 + 1$ and $2 + 1 + 1$ flavor systems; examples are 0.0066 ± 20 [18], 0.013 ± 0.003 [19], 0.0135 ± 0.002 [20], 0.0149 ± 0.0021 [21], 0.020 ± 0.004 [22]. Comparing this with (4.2) and using (4.3), we find $N_c = 1.76$ for $\kappa \sim 0.0153$. This is consistent with the result $N_c \geq 1.2$ obtained in our back reacted case.

In addition, there is the estimation of κ by using the Polyakov-loop extended Nambu–Jona-Lasinio (NJL) model with the mean-field approximation as $\kappa_\chi = 0.017 \pm 0.001$ [23]; it should be noted that this value is estimated from the iso-spin chemical potential but κ should be exactly same in both cases at least in the mean-field approximation. In the case of the PNJL model, there is the estimation of κ for the confinement-deconfinement crossover line as 0.004 ± 0.001 and 0.003 ± 0.001 ; the former one is evaluated from the Polyakov-loop and the later one does the quark number holonomy [24].

5 More about the periodicity

In previous section, we discuss possible connections between lattice QCD simulation near $\mu^2 = 0$. In this section, we discuss deeper properties of the periodicity appearing in QCD. In full QCD, we should have the RW periodicity as explained and demonstrated above. It is, however, well known that we should have the 2π periodicity for $\mu_I/T = \theta$ instead of the Roberge-Weiss (RW) periodicity in the lattice QCD simulation when we fix gauge configurations at $\mu = 0$ or the pure gauge limit where dynamical quarks are not taken into account; later one is corresponding to the quenched limit. In this case, any quantities such as the pressure, the entropy density and the cumulant loses the RW periodicity and thus the minimal period becomes 2π because the grand canonical partition function does not have the RW periodicity. It should be noted that we need the Polyakov-loop phase-flip to consider the RW periodicity in the limits as discussed in Ref. [25, 26].

The 2π periodicity has been used in the calculation of the dual quark condensation. Actual definition of the dual quark condensation is given by

$$\Sigma^{(n)} = \int_0^{2\pi} \frac{d\phi}{2\pi} \sigma(\phi) e^{in\theta} d\phi \quad (5.1)$$

where $\sigma(\phi)$ is the chiral condensate with the phase of the boundary condition, $0 \leq \phi \leq 2\pi$, which is related with the dimensionless imaginary chemical potential as

$$\phi = \theta + \pi. \quad (5.2)$$

In the heavy quark mass regime, it has the clear relation with the Polyakov-loop by using the Dirac mode expansion [5, 6]. Since the dual quark condensate is calculated from the chiral condensate, this quantity may bridge the chiral and the Polyakov-loop dynamics in QCD. Details of the dual quark condensate have been discussed in the lattice QCD simulation [5, 6], the Dyson-Schwinger equation [27], QCD effective models [28, 29, 30]. In principle, we can investigate the Polyakov-loop behavior at $\mu = 0$ from the ϕ -dependent chiral condensate even if calculations of the Polyakov-loop is difficult or impossible.

In the strict probe limit of the holographic model, we also face the same situation of the lattice QCD simulation in the quenched limit; we only has the 2π trivial periodicity. For the consistency between the holographic model and the lattice QCD simulation in both limits, we should reproduce the 2π periodicity in addition to the RW periodicity. Also, it is good to calculate the dual quark condensate in the holographic model to discuss the relation between the chiral condensate and the Polyakov-loop. In addition, if we can understand how to control the boundary condition in the holographic model, we will contact with the \mathcal{Z}_{N_c} twisted QCD; it is an interesting QCD like theory in the viewpoint of the sign problem appearing in the lattice simulation. One possibility to introduce the 2π trivial periodicity in the probe limit is imposing 2π periodic form of θ in the mapping of μ from A_0 : we need the special care for the 2π periodicity issue of the dimensionless imaginary chemical potential.

6 Summary

We have studied here the phase structure and phase transition behaviors ranging from real chemical potential to imaginary one, using a bottom-up holographic model that was introduced to investigate color superconductivity in QCD. From general framework of QCD, one knows that the QCD partition function possesses a certain periodicity, the Roberge-Weiss (RW) periodicity, at the imaginary chemical potential region. Our interest was to see how the analytic continuation of the chemical potential works. To

this end, we have computed the effective potential of the model by including the Kalb-Ramond field in the bulk. Unlike the previous studies based on top-down approach, there is an advantage of our bottom-up approach that one can evaluate the effect of back reaction. As the result, we have observed the RW periodicity as well as the 2π periodicity appropriately. We have further investigated the behavior of the critical line near $\mu = 0$ and tried to see the validity of our analysis. Our results have been compared with those obtained from lattice QCD and effective models such as Polyakov-loop extended NJL model

Acknowledgments

The authors would like to thank helpful discussion with Takeshi Morita. K.K. is supported by the Grants-in-Aid for Scientific Research from JSPS (No. 18K03618).

Appendix

A Roberge-Weiss periodicity in the operator formalism

Since the Roberge-Weiss periodicity must be independent of the gauge fixing condition except the global topology of gauge configuration, the mechanism of the periodicity seems to result strongly from the quark side. In this appendix, we present a brief demonstration of the mechanism in the operator formalism. In the path-integral representation, the periodicity is related to the boundary condition along the imaginary time. Therefore, we omit the spatial degrees of freedom in the following discussions.

Let us begin with a single fermion system. The coherent states are defined by

$$|\xi\rangle = (1 - \xi a^\dagger) |0\rangle = |0\rangle - \xi |1\rangle, \quad \langle\xi| = \frac{1}{i} \langle 0| (\xi - a) = \frac{1}{i} (\langle 0| \xi - \langle 1|) . \quad (\text{A.1})$$

Using the integration rule $\int d\xi \xi = i$, the trace of an operator \mathcal{O} is calculated as

$$\int d\xi \langle\xi| \mathcal{O} |-\xi\rangle = \langle 0| \mathcal{O} |0\rangle + \langle 1| \mathcal{O} |1\rangle = \text{tr } \mathcal{O} . \quad (\text{A.2})$$

This leads to the anti-periodic boundary condition in a path-integral representation [31].

In a particle-antiparticle system, the coherent states which satisfy

$$a |\xi, \bar{\xi}\rangle = \xi |\xi, \bar{\xi}\rangle, \quad b |\xi, \bar{\xi}\rangle = \bar{\xi} |\xi, \bar{\xi}\rangle, \quad \langle\xi, \bar{\xi}| a = \langle\xi, \bar{\xi}| \xi, \quad \langle\xi, \bar{\xi}| b = \langle\xi, \bar{\xi}| \bar{\xi} \quad (\text{A.3})$$

are constructed as follows:

$$|\xi, \bar{\xi}\rangle = (1 - \xi a^\dagger)(1 - \bar{\xi} b^\dagger) |0, 0\rangle = |0, 0\rangle - \xi |1, 0\rangle - \bar{\xi} |0, 1\rangle + \bar{\xi} \xi |1, 1\rangle, \quad (\text{A.4})$$

$$\langle\xi, \bar{\xi}| = \frac{1}{i^2} \langle 0, 0| (\bar{\xi} - b)(\xi - a) = \frac{1}{i^2} (\langle 0, 0| \bar{\xi} \xi + \langle 1, 0| \bar{\xi} - \langle 0, 1| \xi + \langle 1, 1|) . \quad (\text{A.5})$$

Corresponding to boundary conditions as $\psi(\beta) = -\sigma\psi(0)$ and $\bar{\psi}(\beta) = -\sigma^*\bar{\psi}(0)$ in the path-integral representation, the calculation of the trace is modified as

$$\text{tr}_\sigma \mathcal{O} = \int d\xi d\bar{\xi} \langle\xi, \bar{\xi}| \mathcal{O} |-\sigma\xi, -\sigma^*\bar{\xi}\rangle \quad (\text{A.6})$$

$$= \langle 0, 0| \mathcal{O} |0, 0\rangle + \sigma \langle 1, 0| \mathcal{O} |1, 0\rangle + \sigma^* \langle 0, 1| \mathcal{O} |0, 1\rangle + \langle 1, 1| \mathcal{O} |1, 1\rangle \quad (\text{A.7})$$

(This reduces to the normal trace in the case of $\sigma = 1$.)

Note that

$$|-\sigma\xi, -\sigma^*\bar{\xi}\rangle = e^{i\gamma(a^\dagger a - b^\dagger b)} |-\xi, -\bar{\xi}\rangle \quad (\sigma = e^{i\gamma}), \quad (\text{A.8})$$

then we obtain

$$\mathrm{tr}_\sigma \mathcal{O} = \mathrm{tr} (\mathcal{O} e^{i\gamma(a^\dagger a - b^\dagger b)}) . \quad (\text{A.9})$$

Now, the grand potential $Z(\beta, \mu)$ of the $SU(N)$ local gauge theory is invariant under the Z_N transformation associated with the Z_N -twisted boundary condition at $\tau = \beta$ [7]. This is expressed, in the operator formalism, as

$$Z(\beta, \mu) = \sum_A \int [d\xi d\bar{\xi}] \langle A, \xi, \bar{\xi} | \mathcal{O} | A, -\sigma\xi, -\sigma^*\bar{\xi} \rangle , \quad (\text{A.10})$$

in which the label A denotes a set of quantum numbers other than the quark occupation and

$$\langle A, \xi, \bar{\xi} | = \langle A | \left(\bigotimes_{i=1}^N \langle \xi_i, \bar{\xi}_i | \right) , \quad [d\xi d\bar{\xi}] = d\xi_1 d\bar{\xi}_1 \cdots d\xi_N d\bar{\xi}_N , \quad (\text{A.11})$$

$$\mathcal{O} = e^{-\beta(H - \mu \sum_{i=1}^N (a_i^\dagger a_i - b_i^\dagger b_i))} , \quad \sigma = e^{i\frac{2\pi k}{N}} \quad (k \in \{0, 1, \dots, N-1\}) . \quad (\text{A.12})$$

(For simplicity, the degree of freedom associated to the Dirac spinor components is suppressed.) Applying the relation (A.9) and taking account of the commutativity among H , $a_i^\dagger a_i$ and $b_i^\dagger b_i$, one immediately derives the RW periodicity:

$$Z(\beta, \mu) = \sum_A \int [d\xi d\bar{\xi}] \langle A, \xi, \bar{\xi} | e^{-\beta(H - (\mu + i\frac{2\pi k}{\beta N}) \sum_{i=1}^N (a_i^\dagger a_i - b_i^\dagger b_i))} | A, -\xi, -\bar{\xi} \rangle \quad (\text{A.13})$$

$$= Z(\beta, \mu + i\frac{2\pi k}{\beta N}) . \quad (\text{A.14})$$

References

- [1] S. Kobayashi, D. Mateos, S. Matsuura, R. C. Myers and R. M. Thomson, “Holographic phase transitions at finite baryon density,” *JHEP* **0702**, 016 (2007) [hep-th/0611099].
- [2] N. Horigome and Y. Tanii, *Holographic chiral phase transition with chemical potential*, *JHEP* **01** (2007) 072, [hep-th/0608198].
- [3] Kazuo Ghoroku, Kouki Kubo, Motoi Tachibana, Fumihiko Toyoda, ”Holographic cold nuclear matter and neutron star”, *International Journal of Modern Physics A*—Vol. 29, No. 10, 1450060 (2014) , arXiv:1311.1598[hep-th]
- [4] Kazuo Ghoroku, Kouki Kubo, Motoi Tachibana, Tomoki Taminato, Fumihiko Toyoda, ”Holographic cold nuclear matter as dilute instanton gas”, *Phys-RevD*.87.066006, arXiv:1211.2499 [hep-th]
- [5] E. Bilgici, F. Bruckmann, C. Gattringer and C. Hagen, *Phys. Rev. D* **77**, 094007 (2008) doi:10.1103/PhysRevD.77.094007 [arXiv:0801.4051 [hep-lat]].

- [6] E. Bilgici, F. Bruckmann, J. Danzer, C. Gattringer, C. Hagen, E. M. Ilgenfritz and A. Maas, *Few Body Syst.* **47**, 125 (2010) doi:10.1007/s00601-009-0068-x [arXiv:0906.3957 [hep-lat]].
- [7] A. Roberge and N. Weiss, “Gauge theories with imaginary chemical potential and the phases of QCD,” *Nucl. Phys. B* **275**, 734 (1986).
- [8] Gert Aarts, S. Prem Kumar, James Rafferty, ”Holographic Roberge-Weiss Transitions” ,*JHEP* 1007:056,2010, arXiv:1005.2947 [hep-th].
- [9] James Rafferty, ”Holographic Roberge-Weiss Transitions II: Defect Theories and the Sakai-Sugimoto Model” , *JHEP* 1109:087,2011 , arXiv:1103.2315 [hep-th].
- [10] Bigazzi, Francesco and Cotrone, Aldo L., ”Holographic QCD with Dynamical Flavors” , arXiv:1410.2443, [hep-th].
- [11] Hiroshi Isono, Gautam Mandal, Takeshi Morita, ”Thermodynamics of QCD from Sakai-Sugimoto Model” , *JHEP*12(2015)006, arXiv:1507.08949 [hep-th]
- [12] E. Witten, “Anti-de Sitter space, thermal phase transition, and confinement in gauge theories,” *Adv. Theor. Math. Phys.* **2**, 505 (1998) [hep-th/9803131].
- [13] Ofer Aharony, Edward Witten, ”Anti-de Sitter Space and the Center of the Gauge Group2, *JHEP* 9811:018,1998, arXiv:hep-th/9807205
- [14] Kazuo Ghoroku, Kouji Kashiwa, Yoshimasa Nakano, Motoi Tachibana, Fumihiko Toyoda, ”Color Superconductivity in Holographic SYM Theory”, *Phys. Rev. D* **99**, 106011 (2019), arXiv:1902.01093 [hep-th]
- [15] Kazem Bitaghsir Fadafan, Jesus Cruz Rojas, Nick Evans, “A Holographic Description of Colour Superconductivity”, *Phys. Rev. D* **98**, 066010 (2018), [arXiv:1803.03107 [hep-ph]].
- [16] Pallab Basu, Fernando Nogueira, Moshe Rozali, Jared B. Stang, Mark Van Raamsdonk, “Towards A Holographic Model of Color Superconductivity”, *New J.Phys.*13:055001,2011, [arXiv:1101.4042 [hep-th]].
- [17] Massimo D’Elia, Francesco Negro, ”Theta dependence of the deconfinement temperature in Yang-Mills theories”, *PhysRevLett.*109.072001, arXiv:1205.0538 [hep-lat].
- [18] G. Endrodi, Z. Fodor, S. D. Katz and K. K. Szabo, *JHEP* **1104**, 001 (2011) doi:10.1007/JHEP04(2011)001 [arXiv:1102.1356 [hep-lat]].
- [19] C. Bonati, M. D’Elia, M. Mariti, M. Mesiti, F. Negro and F. Sanfilippo, *Phys. Rev. D* **90**, no. 11, 114025 (2014) doi:10.1103/PhysRevD.90.114025 [arXiv:1410.5758 [hep-lat]].

- [20] C. Bonati, M. D’Elia, M. Mariti, M. Mesiti, F. Negro and F. Sanfilippo, Phys. Rev. D **92**, no. 5, 054503 (2015) doi:10.1103/PhysRevD.92.054503 [arXiv:1507.03571 [hep-lat]].
- [21] R. Bellwied, S. Borsanyi, Z. Fodor, Phys. Lett. B **751**, 559 (2015) doi:10.1016/j.physletb.2015.11.011 [arXiv:1507.07510 [hep-lat]].
- [22] P. Cea, L. Cosmai and A. Papa, Phys. Rev. D **93**, no. 1, 014507 (2016) doi:10.1103/PhysRevD.93.014507 [arXiv:1508.07599 [hep-lat]].
- [23] K. Kashiwa and A. Ohnishi, Phys. Lett. B **772**, 669 (2017) doi:10.1016/j.physletb.2017.07.033 [arXiv:1701.04953 [hep-ph]].
- [24] K. Kashiwa and A. Ohnishi, Phys. Rev. D **93**, no. 11, 116002 (2016) doi:10.1103/PhysRevD.93.116002 [arXiv:1602.06037 [hep-ph]].
- [25] T. M. Doi and K. Kashiwa, arXiv:1706.00614 [hep-lat].
- [26] T. M. Doi and K. Kashiwa, EPJ Web Conf. **175**, 12003 (2018) doi:10.1051/epjconf/201817512003 [arXiv:1710.06576 [hep-lat]].
- [27] C. S. Fischer, Phys. Rev. Lett. **103**, 052003 (2009) doi:10.1103/PhysRevLett.103.052003 [arXiv:0904.2700 [hep-ph]].
- [28] K. Kashiwa, H. Kouno and M. Yahiro, Phys. Rev. D **80**, 117901 (2009) doi:10.1103/PhysRevD.80.117901 [arXiv:0908.1213 [hep-ph]].
- [29] F. Xu, H. Mao, T. K. Mukherjee and M. Huang, Phys. Rev. D **84**, 074009 (2011) doi:10.1103/PhysRevD.84.074009 [arXiv:1104.0873 [hep-ph]].
- [30] Phys. Rev. D **88**, no. 7, 077501 (2013) doi:10.1103/PhysRevD.88.077501 [arXiv:1305.6567 [hep-ph]].
- [31] Y. Ohnuki and T. Kashiwa, Prog. Theor. Phys. **60**, 548 (1978).